Heliyon 10 (2024) e26550

Contents lists available at ScienceDirect

Heliyon

journal homepage: www.cell.com/heliyon

Research article

A macrofluidic model to investigate the intrinsic thrombogenicity of clinically used stents and develop less thrombogenic stents

Axelle Y. Kern [a], Yevgeniy Kreinin [b], Lise Charle [a], Mark Epshrein [b], Netanel Korin [b,1], Pierre H. Mangin [a,*,1]

[a] University of Strasbourg, INSERM, EFS Grand-Est, BPPS UMR_S1255, FMTS, F-67065 Strasbourg, France
[b] Department of Biomedical Engineering Technion, Israel Institute of Technology, Haifa, Israel

ARTICLE INFO

Keywords:
Stent
Macrofluidic
Flow chamber
Platelet
Thrombus
Carotid
Femoral
Coronary
Arteries

ABSTRACT

Microfluidic blood flow models have been instrumental to study the functions of blood platelets in hemostasis and arterial thrombosis. However, they are not suited to investigate the interactions of platelets with the foreign surfaces of medical devices such as stents, mainly because of the dimensions and geometry of the microfluidic channels. Indeed, the channels of microfluidic chips are usually rectangular and rarely exceed 50 to 100 μm in height, impairing the insertion of clinically used stents. To fill this gap, we have developed an original macrofluidic flow system, which precisely reproduces the size and geometry of human vessels and therefore represents a biomimetic perfectly suited to insert a clinical stent and study its interplay with blood cells. The system is a circular closed loop incorporating a macrofluidic flow chamber made of silicone elastomer, which can mimic the exact dimensions of any human vessel, including the coronary, carotid or femoral artery. These flow chambers allow the perfect insertion of stents as they are implanted in patients. Perfusion of whole blood anticoagulated with hirudin through the device at relevant flow rates allows one to observe the specific accumulation of fluorescently labeled platelets on the stent surface using video-microscopy. Scanning electron microscopy revealed the formation of very large thrombi composed of tightly packed activated platelets on the stents.

1. Introduction

The occlusion or stenosis of diseased arteries such as the carotid, femoral or coronary artery is often treated by percutaneous transluminal angioplasty. This procedure involves stenting to reopen the vessel and ensures the return to a normal blood flow. While angioplasty with stent implantation has significantly reduced the morbidity and mortality rates related to cardiovascular diseases, one major complication of this procedure is stent thrombosis (ST), which represents an important cause of death post-stenting with mortalities ranging from 10 to 40% [1–4]. The incidence of ST in the coronary arteries has decreased markedly with the use of dual antiplatelet therapy, but the mortality rate is still very elevated and it therefore remains a medical concern that needs to be studied in detail, using refined experimental models [1,5,6]. The thrombi formed on the stents have diverse origins. They can result from the procedure itself, due to stent malposition or fracture, or from the patient's comorbidities, the lesion, a low biocompatibility of the stent, or an inefficient antithrombotic treatment [1,3,7]. This means that the determinants of stent thrombosis are not only the ruptured or

* Corresponding author.
E-mail address: pierre.mangin@efs.sante.fr (P.H. Mangin).
[1] Co-last authors.

https://doi.org/10.1016/j.heliyon.2024.e26550
Received 9 August 2023; Received in revised form 8 February 2024; Accepted 15 February 2024
Available online 22 February 2024
2405-8440/© 2024 The Authors. Published by Elsevier Ltd. This is an open access article under the CC BY-NC license (http://creativecommons.org/licenses/by-nc/4.0/).

eroded atherosclerotic plaque which contains highly thrombogenic material, but also the stent *per se*, notably its design and material.

It has been shown that the materials used to fabricate stents, including stainless steel, tantalum and titanium or cobalt alloys, are thrombogenic as they support platelet adhesion and activation. Indeed, artificial surfaces can adsorb plasma proteins, primarily fibrinogen, which in turn recruit circulating blood cells, mainly platelets [8–10]. Moreover, the stent surface activates the coagulation contact pathway, leading to the generation of thrombin, which is not only the most potent platelet activator, but also transforms fibrinogen into insoluble fibrin, stabilizing the clot that has formed and preventing the blood flow from removing adherent platelets [8]. The design of the stent is another important factor influencing its thrombogenicity, with the strut thickness, number and geometry playing important roles. It has notably been reported that dual-layered stents present a higher rate of ST than single-layered stents, although the underlying mechanism remains poorly defined [11–13].

While some experimental models have been developed to identify the determinants of stent thrombogenicity, they all present major limitations [14–17]. Firstly, they do not reproduce the physiological flow conditions and wall shear rates, since the flow rates used do not mimic the rheological conditions in the relevant arteries. Blood flow is a major factor in hemostasis and thrombosis as it regulates not only platelet functions but also coagulation. Thus, it is probably important to try to reproduce as closely as possible the physiological flows. Another limitation of the current models is that inserting a stent into a straight, smooth and semi-rigid plastic tube does not really mimic the clinical situation, nor the complex flows existing around the stent. Hence, designing flow devices which better reproduce the topography and rigidity of a diseased vessel wall would be a big step forward [10,16–18].

We have developed a device to assess the intrinsic thrombogenicity of clinically used stents. The model relies on the use of flow chambers mimicking the precise geometry of any human vessel, including the coronary, femoral or carotid artery. This device presents the advantage of enabling the easy insertion of a stent into the chamber as it is done in patients. The chamber is then incorporated into a closed circular perfusion system allowing one to perfuse fresh hirudinated whole blood through it at the physiological flow rates found in the aforementioned arteries.

2. Materials and methods

2.1. Resource availability

2.1.1. Lead contact

Requests for resources and additional information should be addressed to Dr Pierre H. Mangin (pierre.mangin@efs.sante.fr).

2.1.2. Data availability statement

Any additional information required to reanalyze the data reported in this paper is available from the lead contact upon request.

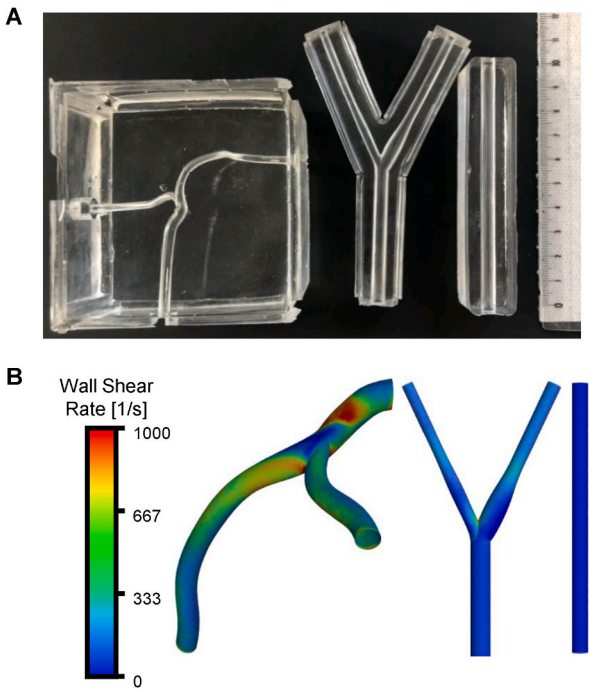

Fig. 1. Macrofluidic flow chambers and their characterization.
(A) Flow chambers modeling the left anterior descending coronary (left), carotid (middle) and femoral (right) arteries and (B) wall shear rate distributions within the models. Wall shear rate distributions were extracted by computational fluid dynamics simulations.

2.2. Experimental model and subject details

All blood donors were healthy volunteers who gave their free and informed written consent to participate in our study, which conformed to the ethical standards of the Declaration of Helsinki. Legal and ethical authorization for the use of blood collected for research was obtained through a national convention between the French National Institute of Health and Medical Research (INSERM) and the French Blood Institute (EFS) (convention number I/DAJ/C2675). Neither the age, nor gender of the donor was recorded.

2.3. Method details

2.3.1. Fabrication of the macrofluidic flow chamber

We use a unique size of common carotid and femoral artery chamber having a diameter of 6 mm. In the case of the coronary artery, the chambers mimic a 4 mm diameter left main coronary artery, a 3 mm diameter circumflex artery and a 3 mm diameter left anterior descending (LAD) artery, which is our artery of focus.

The flow chambers reproduce the average dimensions of human arteries, including the femoral, carotid and coronary arteries (Fig. 1A, Table 1). The chamber is designed with Autodesk Fusion 360 (Autodesk Inc., San Rafael, CA, USA) and a skeleton mimicking the lumen of the artery is printed in 3D with borders using a Form 3 B + printer (Formlabs GmbH, Berlin, Germany). The print supports are removed and the skeleton is sanded with sanding paper P180 and P1000 and polished with "pierre d'argent", composed of clay and soap, cleaned with 70% ethanol to eliminate all sanding residues and lacquered with vanish to obtain the smoothest possible surface. Plastic strips from sheet protectors are glued onto the borders of the skeleton, which is then fixed on a Plexiglas board with acrylic mastic and left overnight at room temperature to avoid any artefacts due to leaking of the material. The chamber is cast with either 45 g of silicone elastomer (Elastosil RT601 A/B, IMCD, Lyon, France) or polydimethylsiloxane (PDMS Sylgard 184, Samaro, Villebon sur Yvette, France) for the carotid and femoral chamber, or 300 g for the coronary chamber. Silicone elastomer has a ratio of 9:1 (W/W) of the components A and B, respectively, component A containing the platinum-based catalyst and component B the polymerization agent. PDMS has a ratio of 10:1 (W/W) of the components A and B, respectively, component A containing the base and component B the curing agent. These materials have the advantage of transparency, which facilitates observation through the walls of the chamber. PDMS is preferred to silicone elastomer if the chamber is to be coated, as the coating ''detaches'' itself from silicone elastomer once the platelet aggregates become too big. The mold is left to dry at room temperature for at least 48 h if made of silicone elastomer, or heated to 70 °C for 3 h if made of PDMS. The chamber is then immersed in acetone to weaken and dissolve the skeleton, for 24–48 h for the femoral and carotid chamber, or for a few days for the coronary chamber because the walls are thicker. Remaining pieces of the skeleton may need to be removed with tweezers, especially at the bifurcation. Thin branches of bamboo are used to remove remaining parts of the skeleton in the coronary chamber, as bamboo is both rigid and flexible enough to pass through the bifurcation in the middle of the chamber.

The wall shear rate maps under these conditions of flow and vessel geometry, extracted using computational fluid dynamics (CFD) simulations (see Supplementary Method), are shown in Fig. 1B and demonstrate the complex shear profiles existing in the carotid, femoral and LAD coronary arteries.

A significant advantage of chambers having the size of human vessels over traditional microfluidic flow chambers is the reproduction of the morphology of human vessels, which allows one to mimic the rheology found in these vessels when using relevant flow rates. However, a major limitation is the volume of blood needed, about 150 mL per perfusion, which implies a limited number of experiments per day for one donor.

2.3.2. Collection of human whole blood

Blood is collected *via* venipuncture from the antecubital vein of consenting healthy volunteers who have not taken any antiplatelet medication during the ten days preceding the donation. An arterio-venous fistula 17G needle is used to obtain a freely running flow. The blood is collected directly into polypropylene Falcon tubes containing 5 mL of a solution of the α-thrombin inhibitor hirudin (final concentration: 100 U/mL) (Transgene, Illkirch-Graffenstaden, France). It is drawn at a reasonably slow and steady rate, taking care to avoid frothing which could activate platelets, and is immediately mixed by gentle inversions of the tube. The first few milliliters of blood are discarded to avoid the effects of traces of thrombin generated during venipuncture. The anticoagulated blood is maintained at physiological temperature (37 °C) in a water bath without agitation and used within 4 h of collection.

Table 1
Dimensions of the macrofluidic flow chambers.

Artery	Internal diameter (mm)	Length (mm)
Common carotid	6	52.5
Internal carotid	4.3	60
External carotid	3.7	60
Femoral	6	100
Left main coronary	3.61	70
Circumflex	2.77	60
Left anterior descending (LAD)	2.8	60

2.3.3. Blocking non-specific platelet interactions with human serum albumin

Whether it has been previously coated or not, the chamber is always passivated to avoid non-specific platelet interactions with the material of the walls. Fatty acid free human serum albumin (HAS 1%) (Sigma-Aldrich, Lyon, France) is injected into the chamber with a Pasteur pipette and left at room temperature for 30 min. To correctly fill the carotid and coronary chambers, it may be necessary to block one vessel while inserting the pipette into another. Once the first two vessels have been filled, one of them is blocked to fill the last one. HSA is later drawn out of the chamber and PBS (supplemented with 2 mM $CaCl_2$ and 1 mM $MgCl_2$) (Sigma-Aldrich) is introduced in the same way as HSA for the time necessary before starting the flow experiment.

2.3.4. Fluorescent labeling of platelets

Monitoring of platelet aggregates and quantitation of thrombus growth by fluorescence macroscopy requires the fluorescent labeling of platelets. The main fluorescent dye used in our laboratory is the lipophilic carbocyanine fluorochrome $DiOC_6$ (3,3′-dihexyloxa-carbocyanine iodide, ThermoFisher Scientific, Illkirch-Graffenstaden, France), which does not cause platelet activation. An additional advantage of this dye is that only platelets and leukocytes are visualized in the presence of red blood cells (RBC), as the fluorescence is quenched by the hemoglobin contained in RBC. Moreover, in a healthy person, the leukocyte count is sufficiently low to be considered as negligible. Platelets are labeled prior to perfusion with $DiOC_6$ by incubation of whole blood at room temperature with 1 μM $DiOC_6$ for 5 min, which corresponds roughly to the time needed to make the last preparations for the flow run.

2.3.5. Basic flow assay

2.3.5.1. Assembly of the perfusion system. The complete perfusion system is shown in Fig. 2 and the various connectors and tubes (Watson-Marlow, La Queue-Lez-Yvelines, France) used to assemble it are depicted in Fig. 3. The tubing used is strong, durable, reusable, easy to clean and does not support non-specific platelet adhesion. .

1. Adjust the pump head to the size of the tubing used (align 6.4 with 1.6 as the internal diameter of the tubing is 6.4 mm, with a wall thickness of 1.6 mm).
2. Put a sheet under the peristaltic pump and near the macroscope to protect it in case of a leak and a black paper under the macroscope to increase the contrast on images.
3. Assemble the system as in Fig. 3 (see Tables 2 and 3 for the tubing and connectors, respectively).

a. Connect tubing 1 with a connector 7.
b. Connect the tubes 2 with the above connector 7 and a second one, respectively.
c. Connect tubing 3 with the above connector 7 and a connector 8 for a carotid or femoral flow chamber. Replace the connector 8 by a connector 9 for the coronary chamber.
d. Assemble the 3-way tap using connectors 10, 11 and 12.

Fig. 2. Macrofluidic perfusion assembly using a carotid artery flow chamber.
The system is composed of a blood reservoir in a water bath at 37 °C and a peristaltic pump perfusing at 380 mL/min through the carotid macrofluidic flow chamber placed on a black paper under a fluorescence macroscope (star *). The blood flows in a closed loop back into the reservoir. A liquid bin is also connected to the flow path and a three-way tap allows one to switch between the bin and the reservoir.

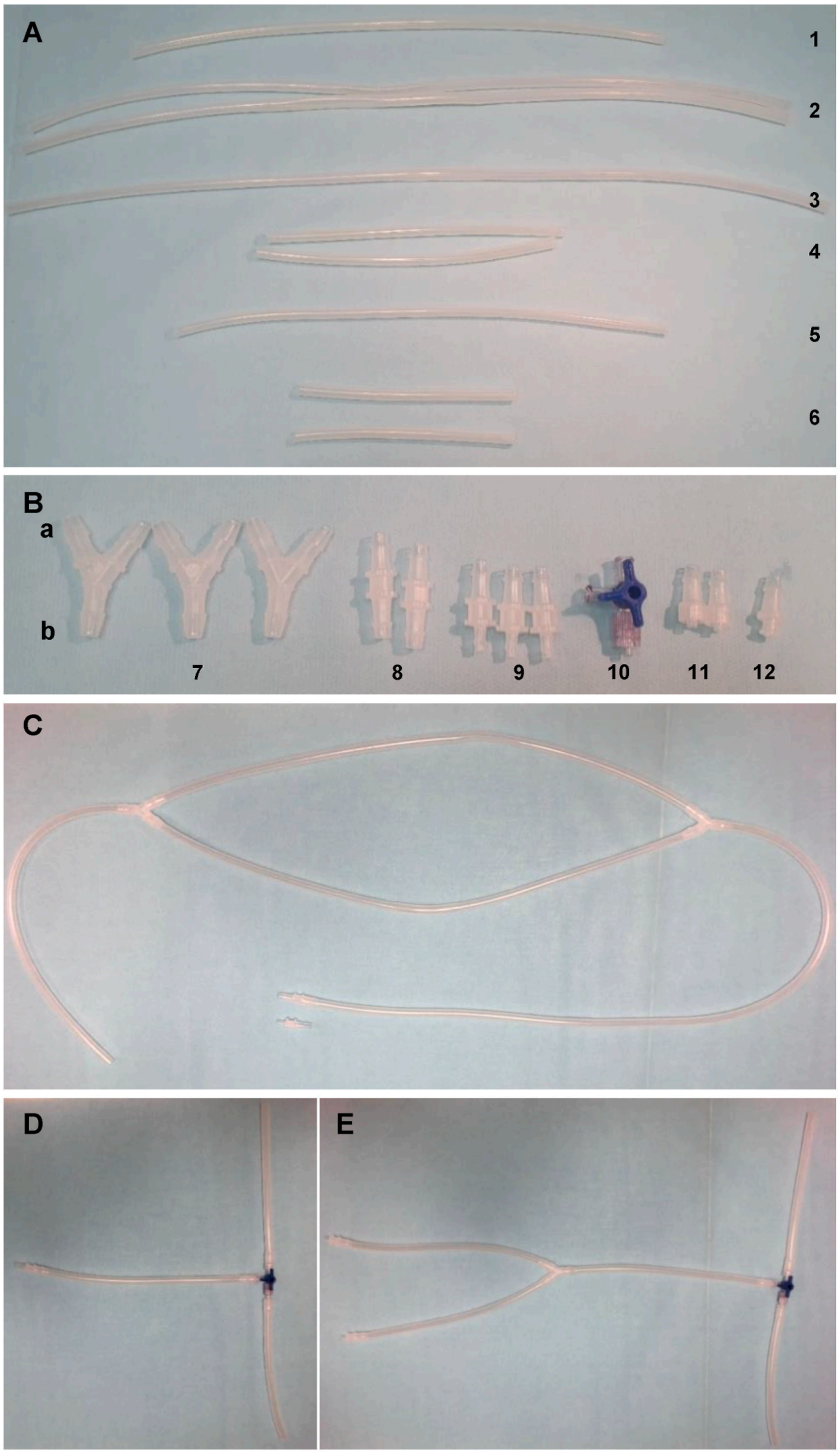

Fig. 3. Tubing and connectors required for the perfusion system.
(A) Tubing and (B) connectors used to assemble the perfusion system. Parts a of the connectors are for the inlet of blood and parts b for the outlet. (C) Perfusion system before the inlet of the flow chamber. The tubes 2 are joined to connectors 7, inlet a. Tubing 1 is connected to the outlet b of one of the connectors 7 and tubing 3 to the other. According to the flow chamber used, tubing 3 is joined to the inlet a of either a connector 8 (carotid and femoral chambers) or a connector 9 (LAD coronary chamber). (D, E) D shows the second part of the femoral chamber. Part a of a connector 8 is connected to the chamber and part b to a tube 4. E depicts the carotid and coronary chambers. The parts a of two connectors 9 are joined to tubes 4. Parts b are connected to the chamber. The three-way tap is assembled and connected to tubing 4 for the middle connector and to tubing 6 on both sides of the tap.

Table 2
Dimensions of the Watson Marlow pumpsil tubing required for the perfusion system.

Tubing n° [a]	Internal diameter (mm)	Wall thickness (mm)	Length required (cm)	Number of tubes required
1	6.4	1.6	40	1
2	6.4	1.6	67	2
3	6.4	1.6	70	1
4	6.4	1.6	25	2
5	6.4	1.6	34	1
6	6.4	1.6	17	2

[a] Refer to Fig. 3A.

Table 3
Dimensions of the connectors required for the perfusion system.

Connector n° [a]	Internal diameter a (inlet) (mm)	Internal diameter b (outlet) (mm)	Number of connectors required
7	6.4	6.4	3
8	6.4	6.4	2
9	6.4	4.8	3
10	6.4	6.4	1
11	6.4	6.4	2
12	6.4	6.4	1

[a] Refer to Fig. 3B.

e. Connect:
   i. Both tubes 4 with a connector 7 and a connector 9 for a carotid or coronary flow chamber.
   ii. One tube 4 with a connector 7 and a connector 8 for a femoral flow chamber.
f. Connect tubing 5 with the above connector 7 and the tap.
g. Join both tubes 6 to the tap to close the system and link to the liquid bin.
h. Insert the stent into the chamber if the experiment requires one. A femoral stent (Lifestent 40 × 8 mm, Bard – Medical Materials, Florida, USA) is placed in the middle of the chamber, a carotid stent (Wallstent Monorail 8 × 29 mm, Boston Scientific S.A.S, France; Casper 8 × 30 mm, Microvention, France), at the bifurcation of the internal and common carotids and a coronary stent (Xience Sierra 4 × 12 mm, Abbott – Medical Materials, Florida, USA) at the bifurcation, mostly in the LAD part and a little in the left coronary artery.
i. Connect the flow chamber to connectors 8 and 9 if necessary.
4. Perfuse PBS through the system to the liquid bin at the flow rate to be used for the experiment, to clean the tubing and connectors. Make sure there are no leaks around the connectors.
5. Stop the flow, replace PBS by the labeled blood and perfuse it to the liquid bin until all PBS has been cleared from the system.
6. Once the whole system has been filled with blood, switch to the closed circuit. Tapping on the tubing and flow chamber allows one to remove air bubbles.
7. Observe the chamber under the macroscope (Leica Z16 APO with plan Apo1/×0.57, Leica Microsystems, Nanterre, France; Orca Fusion Digital Camera C14440, Hamamatsu, USA) to take time-lapse images. Freeze the scale of intensity.

2.3.5.2. Perfusion of blood. Prior to a perfusion assay, establish the required rheological parameters for the given experiment. These include the desired flow rate according to the flow chamber used, the total volume of blood needed and the duration of perfusion. Strict attention should be paid to the volume of blood to be perfused, as a minimum of 150 mL is required. Once the rheological parameters have been established, the required volume of whole blood is carefully transferred to the reservoir of the perfusion assembly, labeled with $DiOC_6$ and stored at 37 °C in the water bath. PBS flow is initiated by starting the peristaltic pump and switching the three-way tap to the PBS reservoir, to ensure cleaning of the system before perfusing blood and check for the absence of leaks. Once 100 mL of PBS has passed, the pump is stopped to change from the PBS to the blood reservoir. The flow rate is set to 380 mL/min for the carotid and 200 mL/min for the femoral and LAD coronary flow chambers, reproducing the average flows found in these arteries [19–21]. Blood flow is then initiated as described above, switching the three-way tap to the blood reservoir. As PBS is susceptible to activate platelets, the first few of milliliters of blood are directed to the liquid bin before the return flow is switched to the reservoir. The perfusion experiment is terminated by continuous perfusion of PBS at the same flow rate to remove all non-adherent cells along with RBC. The majority of non-adherent cells should be flushed from the tubing within 2 min.

2.3.5.3. Cleaning of the perfusion system. At the end of an experiment, all tubes and connectors are filled with FlowClean (Beckmann Coulter, Villepinte, France), left for 20 min and then rinsed with copious volumes of water without detergent and air-dried. Depending on the level of use, the tubing is replaced every two to four months.

2.4. Quantification and statistical analyses

2.4.1. Quantification of platelet aggregates using ImageJ software

The images obtained during time-lapse monitoring and mapping can be analyzed with several different programs, but we use ImageJ software to quantify the fluorescent surface, which corresponds to the platelet aggregates. The edges of the flow chamber to analyze are drawn manually and a measurement is made to obtain the whole area. The threshold is then set to cover the platelet aggregates formed and the area of the aggregates is determined. Any fluorescence outside the drawn edges due to the chamber material is not taken into account. The ratio of the fluorescent area to the total area allows us to quantify and compare the platelet aggregation under different conditions.

2.4.2. Statistics

Results are expressed as the mean ± standard error of the mean. Statistical analyses were performed using GraphPad Prism software (La Jolla, CA, USA). The statistical significance between different groups was assessed using the Kruskal-Wallis test. The p values of <0.05 were considered to be significant ($^*p < 0.05$, $^{**}p < 0.01$).

In Fig. 4C–a Kruskal-Wallis test was performed on 4 of the 5 groups; n was the number of experiments performed and thus the number of stents used. In the control group, n = 10 but one value was excluded after a ROUT test with Q = 0.5% (GraphPad Prism 9.4.1); in the Casper group, n = 6; in the Wallstent group, n = 6; in the Lifestent group, n = 4. The Xience group was too small, n = 2, to perform an analysis.

3. Results

3.1. Monitoring thrombus formation under flow

Areas of observation are defined according to the flow chamber used. We selected specific regions where thrombus formation on stents has been recorded, including the internal carotid artery, the middle of the femoral artery and the bifurcation of the left anterior descending (LAD) coronary artery. However, any other region of the chamber can be imaged either in real-time or at the end of the

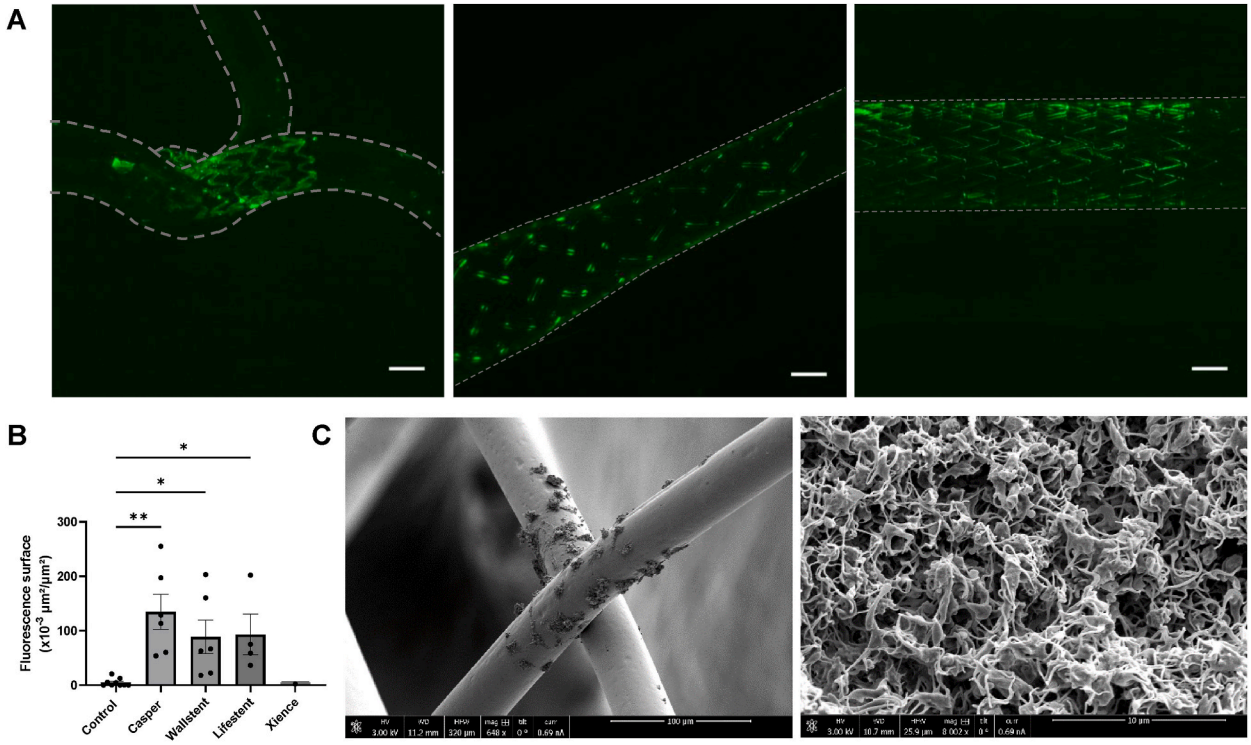

Fig. 4. Images of platelet aggregates on stents.
(A) LAD coronary (left), carotid (middle) and femoral (right) artery stents after perfusion for 1 h with blood labeled with $DiOC_6$. Scale bar: 2 mm. (B) Surface area quantification of platelet aggregation on a carotid stent (Casper and Wallstent), a femoral stent (Lifestent) and a LAD stent (Xience) ($^{**}p = 0.0014$; * Wallstent $p = 0.0139$; * Lifestent $p = 0.319$). Values are the mean ± standard error of the mean. (C) Scanning electron microscopy images of a carotid stent after perfusion with blood for 1 h. Aggregates are observed at the intersection of the stent meshes (left) and are composed of tightly packed activated platelets (right).

experiment. As whole blood is perfused for 1 h, a picture is taken every 15 s in order to observe the growth of the thrombus on the stent. We check for the absence of air bubbles inside the chamber and tubing, before the flow experiment, to avoid air/blood contact which is deleterious and might induce artefacts. To eliminate air bubbles, one can remove them by tapping softly on the tubing and chamber. We also ensure that the outlet tubing is inserted at the bottom of the blood reservoir, so as to always renew the blood. Moreover, the tubing through which blood returns to the reservoir is placed against the reservoir wall to stop the blood "falling" and avoid the risk of platelet activation. When the flow experiment is over, the whole chamber is mapped by taking multiple pictures (Fig. 4A). Quantification is performed over the entire area of the stent (Fig. 4B).

Observation of platelet thrombi using scanning electron microscopy.

Once the whole chamber has been imaged, it is cut open to extract the stent. This step must be performed carefully and the stent should not be manipulated directly to avoid deforming it and thereby damaging the thrombi present on the stent struts. The stent is then placed in a Falcon tube and fixed in 2.5 % glutaraldehyde solution (Electron Microscopy Sciences, Hatfield, Pennsylvania, USA) for at least 1 h at 4 °C. It is important to entirely cover the stent surface with the fixative solution. After removing the fixator and replacing it with cacodylic acid buffer, the tube is placed in a refrigerator at 4 °C. The stent can be conserved for several weeks in this buffer.

To dehydrate it, the stent is first rinsed twice in distilled water, before incubating it in aqueous solutions containing increasing concentrations of ethanol (75%, 80% and 95%), for 5 min each time. The stent is then incubated twice for 20 min in absolute ethanol. It is particularly important not to leave the stent too long in contact with air to avoid its rehydration. Once the stent has been dehydrated, it is placed in solutions composed of hexamethyl-1,1,1,3,3,3-disilazane (HMDS, Sigma-Aldrich) and absolute ethanol: 25% HMDS/75% ethanol, 50% HMDS/50% ethanol and 75% HMDS/25% ethanol, for 5 min each time. Finally, the stent is incubated twice for 5 min in pure HMDS. After drying the stent, sections of interest are cut and fixed on a microscope support with carbon glue. The sections are metallized and examined under a scanning electron microscope (Fig. 4C).

4. Discussion

The macrofluidic flow perfusion system described here enables an accurate and reliable assessment of the intrinsic thrombogenicity of clinically used stents. One major advantage of this model is that it allows us to insert a flow chamber which can mimic any design and therefore reproduce any vascular territory of the human body eligible for stenting, including the carotid, femoral and coronary arteries. A summary of the advantages and disadvantages of our model as compared to pre-existing ones can be found in Table 4. Such a biomimetic chamber enables one to place a stent as it is inserted by a surgeon in a patient. Moreover, applying relevant flow rates in the chamber permits one to faithfully mimic the rheological conditions found in human arteries and should help to better evaluate the importance of rheology in stent thrombosis. In addition, use of pharmacological agents could help to assess the impact of currently used antiplatelet agents on thrombus formation on the stent struts and to define relevant drug concentrations to prevent stent-related thrombosis. This macrofluidic device could also be used to screen new drugs under development and thereby identify novel pharmacological strategies to prevent thrombus formation on stents.

As flow is a recognized major determinant of arterial thrombosis [22–24], our macrofluidic model can be employed to assess the importance of hemodynamics in the thrombogenicity of stents. Thus, by combining experimental flows with CFD around the stent wires, it is possible to precisely define the impact of local rheology on the thrombus formation occurring on the stent. In particular, a better understanding of the importance of the stent-induced flow perturbations triggering thrombosis will open up the possibility of developing novel stents that should be less thrombogenic. Such a device is therefore a relevant and cost-effective experimental model which should be of interest to companies working on new stents. The development of less thrombogenic stents could enable us to adapt therapeutic strategies to use less aggressive antiplatelet therapies and as a consequence, might reduce side effects such as hemorrhages.

Our macrofluidic flow system represents a very attractive platform to evaluate the thrombogenicity of stents under development. Indeed, the existing models present major limitations, notably because they do not reproduce the geometry of human vessels and

Table 4
Advantages and disadvantages of our model as compared to pre-existing ones.

Chandler loop system	• Advantages: permits one to evaluate multiple conditions simultaneously. The passive flow avoids the traumatizing effect of an active pumping system. • Disadvantages: does not allow the insertion of a chamber mimicking the geometry of a vessel, so the pathophysiological conditions found in patients are not faithfully reproduced. The partial filling of the loop creates a large air/fluid interface, which can induce major artefacts.
Annular perfusion chamber	• Advantage: the cylindrical design of the chamber allows the evaluation of stents under laminar blood flow. • Disadvantages: the chamber does not reproduce the geometry of arteries, thus poorly mimicking the clinical situation. The blood is in contact with the external and not the internal side of the stent.
Circular bench-top perfusion model	• Advantage: possibility of combining several systems and therefore testing various conditions at once. • Disadvantage: permits the insertion of a flow chamber but no study appears to have been performed.
Haemobile perfusion system	• Advantage: the rotating motor generates relevant flow rates. • Disadvantage: does not permit the insertion of a flow chamber.
Our closed circuit macrofluidic model	• Advantages: uses a chamber having the dimensions of human arteries. Allows the insertion of a commercial stent as in patients. Relevant rheological conditions can be employed. • Disadvantages: one experiment uses significant amounts of blood and reagent. The peristaltic pump does not reproduce the physiological pulsatile flow.

therefore do not mimic the hemodynamics in human arteries. The thrombogenic potential of new stents is often evaluated in large animal models such as pigs and sheep. Although large animals have the advantage of reproducing both primary and secondary hemostasis, they also entail some important limitations including ethical issues, the elevated costs of large animals and species differences linked to the hemostatic system. Hence the model proposed here represents an interesting screening device which could be applied before testing in animals.

While the design of the chambers described in this work mimics the geometry of healthy vessels based on dimensions reported in the literature, the method can also be used to reproduce diseased vessels since the fabrication relies on a 3D printed scaffold which can easily be adapted. Trying to mimic the topography of diseased vessels could help to better resolve the issues related to stent thrombosis in *in vitro* models and would thus represent an interesting step forward in our understanding of this harmful complication of angioplasty.

The use of living animals has a distinct advantage over *in vitro* flow systems since it better reproduces physiological conditions with the activation of coagulation. Moreover, if experiments are performed *ex vivo* (as in the arterio-venous shunt model), several tubes can be connected in parallel and therefore several conditions may be tested at once, which is not possible using our blood flow assay. However, the *in vitro* macrofluidic system we describe here has numerous advantages including the fact that it does not require a living animal, which is in line with the desired reduction and replacement of animals in scientific research. It is cost-effective as it can generate a useable amount of experimental results at relatively low cost. Another great advantage is that it uses human and not animal blood and therefore avoids species-specific results. Finally, an *in vitro* model allows one to precisely control numerous parameters in order to obtain similar conditions in all experiments.

4.1. Limitations of the model

Although the macrofluidic flow system described here is a new and remarkable model to investigate the intrinsic thrombogenicity of clinically used stents, it still has some limitations.

The first is the use of a peristaltic pump, which produces a semi-constant blood flow instead of a pulsatile flow. An upcoming development would be to use a pulsatile pump in order to better mimic the fluid dynamics in human vessels. This step remains challenging as even in microfluidic studies, the pulsatility is almost never taken into account by the investigators due to technical difficulties. Additionally, the use of connectors integrating more smoothly into the system would allow one to improve the flow transitions in the device.

Another limitation of the macrofluidic flow system is that the chambers do not mimic the rigidity of diseased vessels. It could be interesting to modify the fabrication of the chambers or employ other materials with different rigidity and study the impact on thrombus formation in the stents.

Moreover, the use of hirudinated whole blood does not allow us to evaluate the role of coagulation in thrombus formation on stents as the conditions are non-coagulant. To employ another anticoagulant as in recalcified citrated whole blood could be an interesting development in the close future, but this variant would be complex since coagulation permits thrombus formation throughout the system and could block the blood flow. In the future, lining of the chambers with endothelial cells might also be integrated into the models [25,26].

5. Conclusion

In summary, the model we describe here represents a powerful new platform to evaluate the thrombogenicity of clinically used stents and stents under development and opens up new perspectives to design novel and less thrombogenic stents.

Ethics declaration

This study was reviewed and approved by the French National Institute of Health and Medical Research (INSERM) and the French Blood Institute (EFS) (convention number I/DAJ/C2675). All blood donors provided informed consent to participate in the study.

CRediT authorship contribution statement

Axelle Y. Kern: Writing – review & editing, Writing – original draft, Visualization, Validation, Methodology, Investigation, Formal analysis. **Yevgeniy Kreinin:** Software, Methodology, Formal analysis. **Lise Charle:** Writing – original draft, Validation, Investigation, Formal analysis. **Mark Epshtein:** Software, Methodology, Conceptualization. **Netanel Korin:** Writing – review & editing, Resources, Methodology, Formal analysis, Conceptualization. **Pierre H. Mangin:** Writing – review & editing, Supervision, Resources, Funding acquisition.

Declaration of competing interest

The authors declare that they have no known competing financial interests or personal relationships that could have appeared to influence the work reported in this paper.

Acknowledgements

Funding was provided by the ANR GESTE and the French Federation of Cardiology. The authors acknowledge the helpful support of the Electron Microscopy Team of UMR_S1255 in obtaining high resolution scanning electron microscope images.

Appendix A. Supplementary data

Supplementary data to this article can be found online at https://doi.org/10.1016/j.heliyon.2024.e26550.

References

[1] A. Lotfi, R. Reejhsinghani, Prevention of stent thrombosis: challenges and solutions, VHRM 11 (2015) 93–106, https://doi.org/10.2147/VHRM.S43357.
[2] T.E. Watts, A. Chatterjee, M.A. Leesar, Stent thrombosis: early, late, and very late, in: Cardiovascular Thrombus, Academic Press, 2018, pp. 217–224.
[3] J. Torrado, L. Buckley, A. Durán, P. Trujillo, S. Toldo, J. Valle Raleigh, A. Abbate, G. Biondi-Zoccai, L.A. Guzmán, Restenosis, stent thrombosis, and bleeding complications, J. Am. Coll. Cardiol. 71 (2018) 1676–1695, https://doi.org/10.1016/j.jacc.2018.02.023.
[4] D.E. Cutlip, D.S. Baim, K.K.L. Ho, J.J. Popma, A.J. Lansky, D.J. Cohen, J.P. Carrozza, M.S. Chauhan, O. Rodriguez, R.E. Kuntz, Stent thrombosis in the modern era, Circulation 103 (2001) 1967–1971, https://doi.org/10.1161/01.cir.103.15.1967.
[5] R. Pop, I. Zinchenko, V. Quenardelle, D. Mihoc, M. Manisor, J.S. Richter, F. Severac, M. Simu, S. Chibbaro, O. Rouyer, et al., Predictors and clinical impact of delayed stent thrombosis after thrombectomy for acute stroke with tandem lesions, AJNR Am. J. Neuroradiol. (2019), https://doi.org/10.3174/ajnr.A5976 ajnr; ajnr.A5976v1.
[6] K. Katsanos, S.A.M. Al-Lamki, A. Parthipun, S. Spiliopoulos, S.D. Patel, I. Paraskevopoulos, H. Zayed, A. Diamantopoulos, Peripheral stent thrombosis leading to acute limb ischemia and major amputation: incidence and risk factors in the aortoiliac and femoropopliteal arteries, Cardiovasc. Intervent. Radiol. 40 (2017) 351–359, https://doi.org/10.1007/s00270-016-1513-0.
[7] A.J. Kirtane, G.W. Stone, How to minimize stent thrombosis, Circulation 124 (2011) 1283–1287, https://doi.org/10.1161/CIRCULATIONAHA.110.976829.
[8] I.H. Jaffer, J.C. Fredenburgh, J. Hirsh, J.I. Weitz, Medical device-induced thrombosis: what causes it and how can we prevent it? J. Thromb. Haemostasis 13 (2015) S72–S81, https://doi.org/10.1111/jth.12961.
[9] K. Kolandaivelu, R. Swaminathan, W.J. Gibson, V.B. Kolachalama, K.-L. Nguyen-Ehrenreich, V.L. Giddings, L. Coleman, G.K. Wong, E.R. Edelman, Stent thrombogenicity early in high-risk interventional settings is driven by stent design and deployment and protected by polymer-drug coatings, Circulation 123 (2011) 1400–1409, https://doi.org/10.1161/CIRCULATIONAHA.110.003210.
[10] M.U. Zafar, J.J. Bravo-Cordero, S. Torramade-Moix, G. Escolar, D. Jerez-Dolz, E.I. Lev, J.J. Badimon, Effects of electret coating technology on coronary stent thrombogenicity, Platelets 33 (2022) 312–319, https://doi.org/10.1080/09537104.2021.1912313.
[11] J.A.R. Pfaff, C. Maurer, E. Broussalis, H. Janssen, R. Blanc, C. Dargazanli, V. Costalat, M. Piotin, F. Runck, A. Berlis, et al., Acute thromboses and occlusions of dual layer carotid stents in endovascular treatment of tandem occlusions, J. NeuroIntervent. Surg. 12 (2020) 33–37, https://doi.org/10.1136/neurintsurg-2019-015032.
[12] U. Yilmaz, H. Körner, R. Mühl-Benninghaus, A. Simgen, C. Kraus, S. Walter, S. Behnke, K. Faßbender, W. Reith, M.M. Unger, Acute occlusions of dual-layer carotid stents after endovascular emergency treatment of tandem lesions, Stroke 48 (2017) 2171–2175, https://doi.org/10.1161/STROKEAHA.116.015965.
[13] T. Klail, C. Kurmann, J. Kaesmacher, A. Mujanovic, E.I. Piechowiak, T. Dobrocky, S. Pilgram-Pastor, A. Scutelnic, M.R. Heldner, J. Gralla, et al., Safety and efficacy of carotid artery stenting with the CGuard double-layer stent in acute ischemic stroke, Clin. Neuroradiol. 33 (2023) 237–244, https://doi.org/10.1007/s00062-022-01209-3.
[14] A.B. Chandler, In vitro thrombotic coagulation of the blood; a method for producing a thrombus, Lab. Invest. 7 (1958) 110–114.
[15] K.S. Sakariassen, P.A. Aarts, P.G. de Groot, W.P. Houdijk, J.J. Sixma, A perfusion chamber developed to investigate platelet interaction in flowing blood with human vessel wall cells, their extracellular matrix, and purified components, Lab. J. Clin. Med. 102 (1983) 522–535.
[16] C. Beythien, W. Terres, C.W. Hamm, In vitro model to test the thrombogenicity of coronary stents, Thromb. Res. 75 (1994) 581–590, https://doi.org/10.1016/0049-3848(94)90170-8.
[17] G.E. Engels, S.L.J. Blok, W. van Oeveren, *In vitro* blood flow model with physiological wall shear stress for hemocompatibility testing—an example of coronary stent testing, Biointerphases 11 (2016) 031004, https://doi.org/10.1116/1.4958979.
[18] G. Tepe, J. Schmehl, H. P Wendel, S. Schaffner, S. Heller, M. Gianotti, C. D Claussen, S. H Duda, Reduced thrombogenicity of nitinol stents—in vitro evaluation of different surface modifications and coatings, Biomaterials 27 (2006) 643–650, https://doi.org/10.1016/j.biomaterials.2005.06.004.
[19] H. Wieneke, C. von Birgelen, M. Haude, H. Eggebrecht, S. Möhlenkamp, A. Schmermund, D. Böse, C. Altmann, T. Bartel, R. Erbel, Determinants of coronary blood flow in humans: quantification by intracoronary Doppler and ultrasound, J. Appl. Physiol. 98 (2005) 1076–1082, https://doi.org/10.1152/japplphysiol.00724.2004.
[20] H.-L. Liang, Doppler flow measurement of lower extremity arteries adjusted by pulsatility index, Am. J. Roentgenol. 214 (2020) 10–17, https://doi.org/10.2214/AJR.19.21280.
[21] A. Benetos, A. Simon, J. Levenson, P. Lagneau, J. Bouthier, M. Safar, Pulsed Doppler: an evaluation of diameter, blood velocity and blood flow of the common carotid artery in patients with isolated unilateral stenosis of the internal carotid artery, Stroke 16 (1985) 969–972, https://doi.org/10.1161/01.STR.16.6.969.
[22] W.S. Nesbitt, P. Mangin, H.H. Salem, S.P. Jackson, The impact of blood rheology on the molecular and cellular events underlying arterial thrombosis, J. Mol. Med. 84 (2006) 989–995, https://doi.org/10.1007/s00109-006-0101-1.
[23] W.S. Nesbitt, E. Westein, F.J. Tovar-Lopez, E. Tolouei, A. Mitchell, J. Fu, J. Carberry, A. Fouras, S.P. Jackson, A shear gradient–dependent platelet aggregation mechanism drives thrombus formation, Nat. Med. 15 (2009) 665–673, https://doi.org/10.1038/nm.1955.
[24] M.H. Kroll, J.D. Hellums, Platelets and shear stress, Blood 88 (1996) 1525–1541, https://doi.org/10.1182/blood.V88.5.1525.1525.
[25] M. Khoury, M. Epshtein, H. Zidan, H. Zukerman, N. Korin, Mapping deposition of particles in reconstructed models of human arteries, J. Contr. Release 318 (2020) 78–85, https://doi.org/10.1016/j.jconrel.2019.12.004.
[26] M. Khoury, M. Epshtein, N. Korin, In vitro 3D cell-cultured arterial models for studying vascular drug targeting under flow, J. Vis. Exp. 14 (2021), https://doi.org/10.3791/62279.